Angewandte Chemie
Eine Zeitschrift der Gesellschaft Deutscher Chemiker

Supporting Information

Inverted Wedding Cake Growth Operated by the Ehrlich–Schwoebel Barrier in Two-Dimensional Nanocrystal Evolution

*Xin Yin, Dalong Geng, and Xudong Wang**

anie_201510376_sm_miscellaneous_information.pdf

Methods

5 g zinc oxide powder was weighed as the precursor and loaded in an alumina boat. The boat was then placed at the center of an alumina tube located inside a single-zone tube furnace. Argon carrier gas with the flow rate of 50 sccm was applied and the pressure inside the tube was kept at 53 Pa. Three polycrystalline alumina substrates (11.4 cm in length and 1 cm in width) were lined together in the tube which covered a broad deposition temperature. The system temperature reached 1273 K during the first 40 minutes and reached 1673 K after another 50 minutes. The precursor completely decomposed and vaporized before the temperature reached 1673 K. Subsequently, the system was cooled down to room temperature naturally under the same argon atmosphere.

Zeiss LEO 1530 Schottky-type field-emission scanning electron microscope was used to study the morphologies of the samples. FEI TF30 transmission electron microscope operated at 300 kV was used to study the crystal structure of the samples. Atomic force microscopy (AFM) tomography images were obtained using XE-70 Park Systems. Zeiss 1540XB CrossBeam Focused Ion Beam FE SEM was used to cut the plate-capped NW structure by the flux of gallium ions along the axis of the rod. Because ions flux may damage the surface feature, a carbon layer and a platinum layer were deposited on the sample for protection of the surface feature.

S1. Plenty of morphologies featured by basin-shaped crown caped NWs.

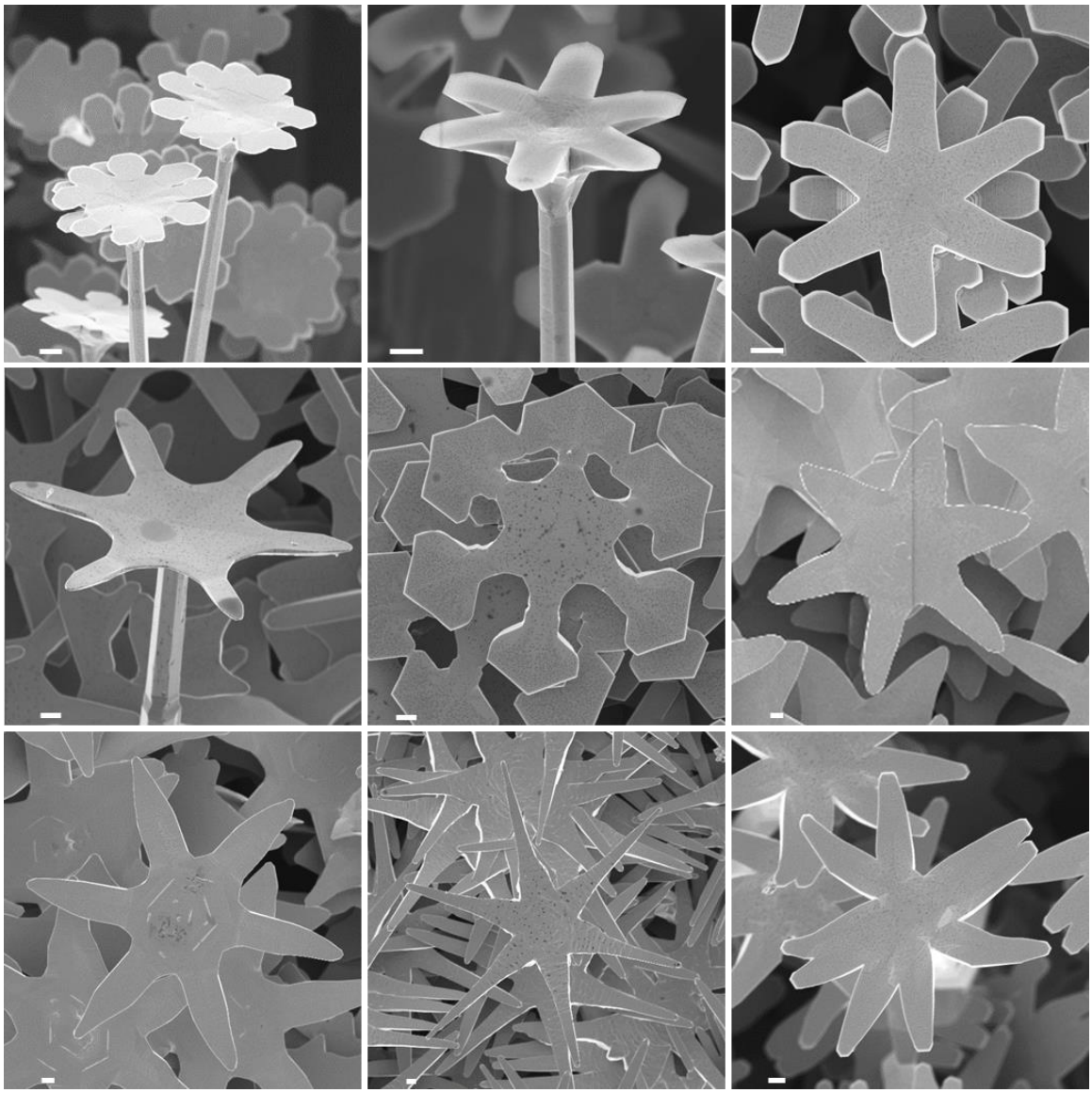

Figure S1. Using different growth kinetics (different deposition temperatures, and different oxygen partial pressures), plenty of branch-caped NWs with different features were obtained. The scale bars are 1 μm.

S2. Evolution of plate morphology influenced by deposition temperatures and oxygen partial pressures.

SEM images show the plate morphology evolution with deposition temperatures and oxygen partial pressures in the large scale. The detailed morphologies of individual plates are presented in Figure 4B in the main text accordingly. Each plate morphology exhibits good uniformity within a relative large area (~0.1-1 mm on the substrate) where the deposition conditions are nearly identical.

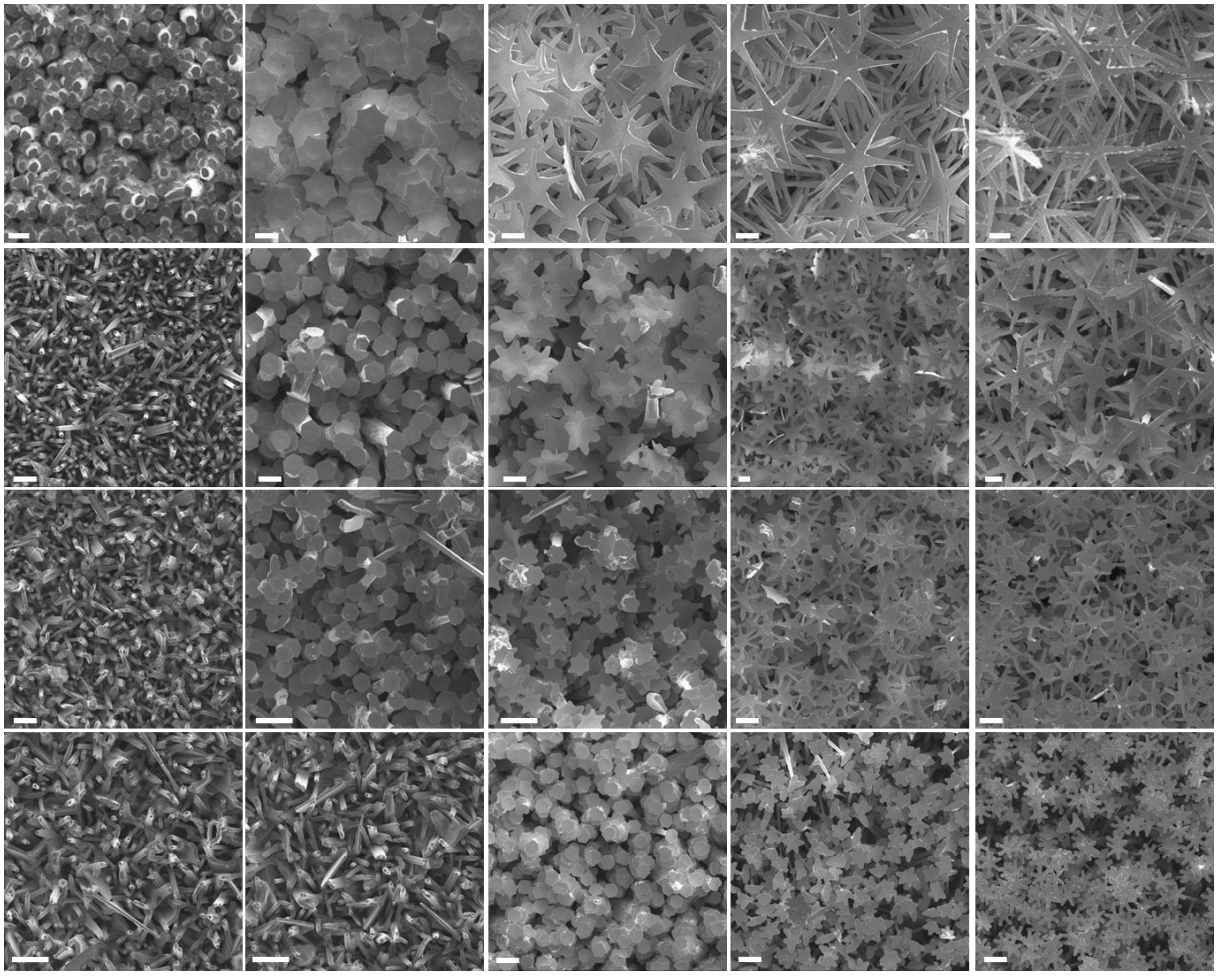

Figure 2. Large scale SEM images from the experiments with different oxygen partial pressures. The deposition temperature decreases from left to right. The oxygen partial pressures decreases from top to bottom: 50 Pa (1st row), 30 Pa (2nd row), 10 Pa (3rd row), and 1 Pa (4th row). The scale bars are 10 μm.

S3. Change of the equilibrium pressure and real pressure along the chamber during the increase of the chamber temperature

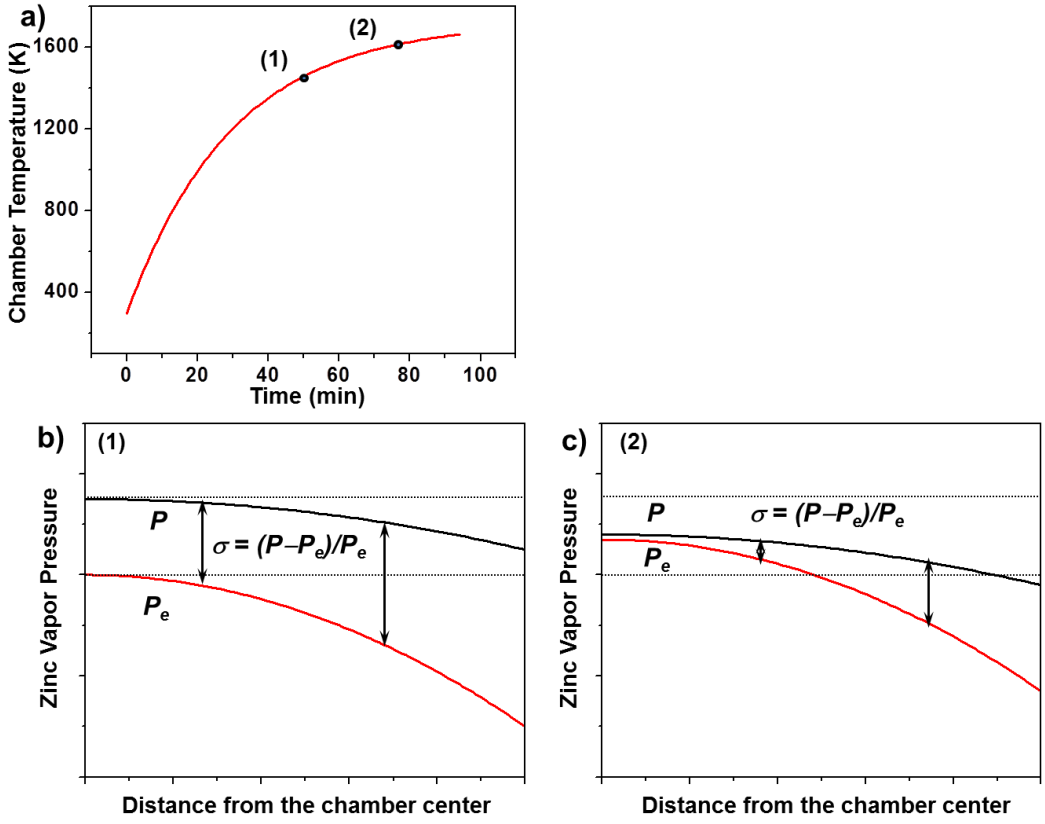

Figure 3. a) Increase of chamber temperature with time. Equilibrium pressure (P_e) and real pressure (P) variation with the distance from the chamber center at chamber temperature 1 (b) and 2 (c) labeled in (a).

S4. Measurement of the Ehrlich-Schwoebel barrier energy

S4.1. Diffusion down rate derivation

The diffusion down rate can be written as[1]

$$v_d = a\frac{a}{\delta_0}(j_+ - j_-)\exp(-\frac{E_{ES} - E_{sd}}{kT}) \quad \text{(S1)}$$

where v_d is the diffusion down rate, a is the lattice constant, δ_0 is the kink spacing, a/δ_0 is the probability to find a kink site, and j_+ and j_- are the fluxes of attachment and detachment of building units per site of growth to and from the growing surface, respectively. The exponential term indicates the diffusion down probability, where E_{SE} is the SE barrier energy, and E_{sd} is the surface diffusion barrier energy.[2] j_+ and j_- are expressed as[1]

$$j_+ = \frac{P}{\sqrt{2\pi mkT}}a^2\exp(-\frac{\Delta U}{kT}) \quad \text{(S2)}$$

$$j_- = \frac{P_e}{\sqrt{2\pi mkT}}a^2\exp(-\frac{\Delta U}{kT}) \quad \text{(S3)}$$

where ΔU is kinetic barrier for the incorporation of the building units into the half crystal.

Insert Eq. S2 and S3 into Eq. S1, we can get

$$v_d = \frac{a^4}{\delta_0}\frac{P - P_e}{\sqrt{2\pi mkT}}\exp(-\frac{E_{ES} - E_{sd} + \Delta U}{kT}) \quad \text{(S4)}$$

In order to express v_d in term of temperature, such conversions below are used

$$P - P_e = \sigma P_e \approx 3654 \times \exp(\frac{8340}{T}) \quad \text{(S5)}$$

$$T^{-1/2} \approx 0.01568 \times \exp(\frac{747.7}{T}) \quad \text{(S6)}$$

Insert Eq. S5 and S6 into Eq. S4, the diffusion down rate can be expressed below,

$$v_d = \frac{57.3a^4}{\delta_0\sqrt{2\pi mk}}\exp(-\frac{\frac{E_{ES} - E_{sd} + \Delta U}{k} - 747.7 - 8340}{T}) \quad \text{(S7)}$$

Take the natural logarithm at both sides, the diffusion down rate becomes

$$\ln v_d = \ln(\frac{57.3a^4}{\delta_0\sqrt{2\pi mk}}) - (\frac{E_{ES} - E_{sd} + \Delta U}{k} - 9087.7)\frac{1}{T} \quad \text{(S8)}$$

Thus, by plotting $\ln v_d$ versus $1/T$, we can get the value of E_{ES}–E_{sd} from the slope.

S4.2. Plot lnv_d as a function of *1/T*

The ratio between the axial growth rate and the diffusion down rate can be presented by the ratio of plate thickness (*s*) to suspended length of plate (*l*), as shown below

$$\frac{s}{l} = \frac{v_a t}{v_d t} = \frac{v_a}{v_d} \tag{S9}$$

Thus, the diffusion down rate can be written in term of v_a as

$$v_d = \frac{l}{s} v_a \tag{S10}$$

where v_a can be estimated by considering the nanostructure length along the axial direction and the time taken to reach such a length. Thus, through measuring the thickness *s*, the suspended length of plate *l*, and calculating v_a, v_d can be obtained. Combining with the measured temperature according to the sample positions, the relationship between lnv_d and 1/T can be plotted.

Reference

[1] I. V. Markov, *Crystal Growth For Beginners: Fundamentals of Nucleation, Crystal Growth and Epitaxy (World Scientific, Singapore, 2003)*.

[2] a) W. K. Burton, N. Cabrera, C. Frank, *Philos. Tr. Soc. S.-A* **1951**, *243*, 299-358; b) X. Yin, J. Shi, X. Niu, H. Huang, X. Wang, *Nano Lett.* **2015**, *15*, 7766-7772.